A dynamic probabilistic safety margin characterization approach in support of Integrated Deterministic and Probabilistic Safety Analysis

Francesco Di Maio, Ajit Rai, Enrico Zio

HAL Id: hal-01786979
https://hal.science/hal-01786979

Submitted on 23 Mar 2020

A DYNAMIC PROBABILISTIC SAFETY MARGIN CHARACTERIZATION APPROACH IN SUPPORT OF INTEGRATED DETERMINISTIC AND PROBABILISTIC SAFETY ANALYSIS

Francesco Di Maio[a], Ajit Rai[b], Enrico Zio[a,c]
[a]Energy Department, Politecnico di Milano, Via La Masa 34, 20156 Milano, Italy
francesco.dimaio@polimi.it
[b]Grenoble Institute of Technology- PHELMA, Grenoble, France
[c] Chair on System Science and Energetic Challenge
Fondation EDF, Ecole Centrale and Supelec, Paris, France

ABSTRACT

The challenge of Risk-Informed Safety Margin Characterization (RISMC) is to develop a methodology for estimating system safety margins in presence of stochastic and epistemic uncertainties affecting the system dynamic behavior. This is useful to support decision-making for licensing purposes. In the present work, safety margin uncertainties are handled by Order Statistics (OS) (with both Bracketing and Coverage approaches) to jointly estimate percentiles of the distributions of the safety parameter and of the time required for it to reach these percentiles values during its dynamic evolution. The novelty of the proposed approach consists in the integration of dynamic aspects (i.e., timing of events) into the definition of a dynamic safety margin for a probabilistic Quantification of Margin and Uncertainties (QMU). The system here considered for demonstration purposes is the Lead- Bismuth Eutectic- eXperimental Accelerator Driven System (LBE-XADS).

Keywords: Risk-Informed Safety Margins; Dynamic Probabilistic Safety Margins; Order Statistics; Grace time.

NOTATION AND LIST OF ACRONYMS

BDBA	Beyond Design Basis Accident
BE	Best Estimate
DBA	Design Basis Accident
DET	Dynamic Event Tree
DSA	Deterministic Safety Analysis
DSM	Dynamic probabilistic Safety Margin
ECCS	Emergency Core Cooling System
ET	Event Tree
FT	Fault Tree
IDPSA	Integrated Deterministic & Probabilistic Safety Assessment
LBE-XADS	Lead Bismuth Eutectic- eXperimental Accelerator Driven System
LOCA	Loss Of Coolant Accident
MC	Monte Carlo
NPP	Nuclear Power Plant
OS	Order Statistics

PCT	Peak Cladding Temperature
PID	Proportional- Integral-Derivative controller
PSA	Probabilistic Safety Assessment
PWR	Pressurized Water Reactor
QMU	Quantification of Margin and Uncertainties
RISMC	Risk Informed Safety Margin Characterization
TH	Thermal Hydraulic
U	Upper Safety Threshold
L	Lower Safety Threshold
$T_{o,max}$	Maximum Temperature of Diathermic Oil
$P(t)$	Thermal power
$Q(t)$	Proton Beam
$\tau_{LB}^{C,P}$	Temperature of LBE liquid leaving from the top of the core of the LBE XADS
$\tau_{LB}^{P,C}$	Temperature of LBE liquid re-entering the core from the bottom of the LBE XADS
$T_{LB}^{av,C}$	Average in-core temperature of LBE liquid
$\Gamma_a(t)$	Airflow
$T_o^{av,S}$	Average temperature of diathermic oil
$T_o^{th,u}$	Upper safety threshold of LBE XADS diathermic oil temperature
$T_o^{th,l}$	Lower safety threshold of LBE XADS diathermic oil temperature
m_1	Flow rate of air when PID controller fails stuck
m_2	Airflow mass flow when air coolers fail stuck
m_3	Flow rate of air when feedforward controller fails stuck
Ta_{in}	Air inlet temperature from air cooler
$\bar{x}$	Input values vector
x_m	m^{th} element of the input vector
$\bar{x}^{(i)}$	i^{th} element of the representative sample of independent input vectors
J	Number of safety parameters
j	Index of the safety parameter
y	Set of values of first output vector (e.g., safety parameter)
$y_j(a)$	j-th safety parameter for accidental scenario a
y_{jref}	Reference value for $y_j(a)$
$M(y_j, a)$	Safety margin for the j-th safety parameter during accidental scenario a
$M(\gamma, \beta)$	Probabilistic safety margin
$M(\gamma_1, \gamma_2, \beta_1, \beta_2)$	Dynamic probabilistic safety margin
y	Set of values of first output vector (e.g., safety parameter)
y_t	Set of values of second output vector (e.g., time)
$\bar{y}$	Safety parameter output vector
$\bar{y}^*$	Ordered set of the safety parameter output vector
$\bar{y}_t$	Time output vector
$\bar{y}_t^*$	Ordered set of the time output vector
$f(y)$	Probability density function of y
$f(y_\gamma)$	Probability density function of the γ-th percentile of y
k	Number of outputs
N	Number of simulations
β	Confidence value
β_1	Confidence value of the safety parameter (e.g., 95%)
β_2	Confidence value of the time (e.g., 95%)
γ	Coverage value

γ_1	Coverage value of the safety parameter (e.g., 95th percentile)
γ_2	Coverage value of the time (e.g., 5th percentile)
m	Number of values that lie beyond the γ coverage extent
y_γ	Real γ^{th} percentile
$\hat{y}_{\gamma_1}$	Estimated γ^{th} percentile of the safety parameter
$\hat{y}_{t_{\gamma_2}}$	Estimated γ^{th} percentile of the time
y_{γ_1}	Real value of the γth percentile of the safety parameter
$y_{t_{\gamma_2}}$	Real value of the γth percentile of the time
y_{95}	Real 95th percentile
$\hat{y}_{95}$	Estimate of the 95th percentile

1. INTRODUCTION

Risk assessment and safety analysis are traditionally supported by a Deterministic Safety Analysis (DSA) of a limited set of Design Basis Accidents (DBAs) under largely conservative assumptions [NUREG CR-6042, U.S. NRC, 1994]. For this, IAEA defines four possible options that combine differently computer codes availability, realism of assumptions and boundary conditions [IAEA SSG-2, 2008]. Among these options, traditional DSA using Best Estimate (BE) Thermal-Hydraulic (TH) codes based on conservative (pessimistic) assumptions on the system dynamics and physical models (i.e., IAEA option 3) is limited in the consideration of system failure modes and sequences, timing and order of failure events.

Probabilistic Safety Assessment (PSA) overcomes the limitation of considering only DBAs by extending the set of accidents through a systematic analysis of the failure events and sequences (e.g., by Event Trees (ETs) / Fault Trees (FTs)). Yet, PSA does not give full account to the timing of failure events and to the magnitude of component failures, which can be important especially when the system dynamics significantly influences the system failure behavior [Rutt et al., 2006].

Dynamic reliability approaches [Siu, 1994; Devooght, 1997; Marseguerra et al., 1998; Labeau et al., 2000; Dufour et al., 2002; Di Maio et al., 2009; Aldemir, 2013] have been developed, aimed at giving explicit account to the interactions among the physical parameters of the process (such as temperature, pressure, speed, etc.), the human

operators actions and the failures of the hardware and software components. This creates the opportunity of DSA and PSA integration into one framework of Integrated Deterministic and Probabilistic Safety Analysis (IDPSA) [Aldemir, 2013; Zio, 2014] and as a by-product for the quantification of operational safety margins within a dynamic reliability scheme [Zio et al., 2012].

Traditionally, a safety margin is defined as the minimum distance between the system "loading" and its "capacity" [US D.O.E., 2009]. The challenge is the effective representation of the uncertainties inherent in the TH code parameters, correlations and approximations.

Uncertainty is typically distinguished into two types: randomness due to inherent variability in the system behavior and imprecision due to lack of knowledge and information on the system [Apostolakis, 1990]. The former type of uncertainty is often referred to as objective, aleatory, stochastic, whereas the latter is often referred to as subjective, epistemic, state of knowledge [Apostolakis 1990; Helton, 2011]. To deal with these uncertainties, traditional safety margins quantification in DSA analysis has implied conservatism in both the analysis of the TH code outputs and the evaluation criteria [Nutt et al., 2004]. Best Estimate (BE) methodologies have reduced the amount of conservatism for the evaluation of safety margins, but do not take into account all aleatory and epistemic uncertainties in the physical models stochastic behavior and model parameter values [US D.O.E., 2009].

In order to more realistically quantify the uncertainty of TH code outcomes, a probabilistic safety margin definition has been proposed for PSA, which better deals with epistemic uncertainties [Zio et al., 2010]. However, the effect of timing, order and magnitude of the component failures on the system dynamics is not considered.

In this respect, a Dynamic probabilistic Safety Margin (DSM) approach is proposed in this paper, based on time-dependent phenomenological models of stochastic system evolution including possible dependencies between failure events [Aldemir, 2013]. For this, we introduce a novel definition of a DSM by the combined quantification of a percentile (e.g., 95th) of the safety parameter distribution (e.g., oil temperature, peak cladding temperature) and a percentile (e.g., 5th) of the distribution of the earliest time required to the safety parameter to reach the given percentile value. The uncertainties

affecting the DSM are treated using Order Statistics (OS) (i.e., Bracketing and Coverage approach) [Nutt et al., 2004]. By doing so, we are able to compute the confidence that, for a selected accidental scenario of a Dynamic Event Tree (DET) obtained by a IDPSA analysis, the estimated 95th percentile of the safety parameter cannot be reached before the 5th percentile of the estimated time: if these estimated percentiles meet the safety criteria with the required confidence, the NPP can be licensed as "safe" to withstand the selected accidental scenario.

The rationale behind the choice of the selection of the 95th and the 5th percentiles for the safety parameter and the estimated time, respectively, lies in the attempt of assuring that there is no significant evidence of exceedance of the safety parameter threshold which could lead to a higher than accepted probability of failure within an extremely unavoidable (fast) time (i.e., the unlikely condition that the safety parameter reaches the threshold within the 5th percentile value of the time distribution). With these assumptions, the proposed definition of DSM provides the analyst with the additional resilience information on the available time for counteracting the occurrence of an accidental scenario, rather than only quantifying to which extent the selected combination of failure events can be harmful for the NPP.

The proposed framework of analysis is developed with reference to a Lead Bismuth Eutectic-eXperimental Accelerator Driven System (LBE-XADS) model, in which the average oil temperature ($T_o^{av,S}$), of the secondary coolant loop is taken as the safety parameter [Cammi et al., 2006; Di Maio et al., 2009]. A SIMULINK model of the LBE-XADS system is used for the estimation of the percentiles of the maximum oil temperature ($T_{o,max}$) distribution and of the distribution of the time required to reach $T_{o,max}$. A Monte Carlo (MC)-driven fault injection engine is used for randomly sampling the model parameters values, the components failures times and magnitudes. The illustration of the analysis is given with respect to one accidental scenario of a DET generated in an IDPSA.

The paper is organized as follows. In Section 2, the concept of probabilistic safety margin is explored and that of DSM is introduced. In Section 3, a brief explanation is given of the OS approaches (bracketing and coverage) used for the definition of the number of TH code runs for uncertainty analysis with a required confidence (e.g., 95%) in the

quantification of the DSM. In Section 4, a short description of the LBE-XADS system and its failure modes is given, along with the SIMULINK model used. The MC driven fault injection engine, used for sampling the physical parameters affecting the system behavior (epistemic uncertainties) and the components failure times and magnitudes (aleatory uncertainties), is also presented, the effects of the uncertainties on the dynamic evolution of $T_{o,max}$ are discussed, and the results are shown and analyzed. Conclusions of the whole study are drawn in Section 5.

2. DYNAMIC PROBABILISTIC SAFETY MARGIN

Traditionally, for an accidental scenario 'a', the safety margin $M(y_j, a)$ is defined as the difference between the conservatively computed values reached by a selected safety parameter $y_j(a)$, j=1,2,…J, and a predefined upper (lower) threshold U_j (L_j) during an accidental scenario [Nutt et al., 2004; Secchi et al., 2008; Martorell et al., 2009].
For the upper threshold U_j, it is defined as:

$$M(y_j, a) = \begin{cases} \dfrac{U_j - y_j(a)}{U_j - y_{j\,ref}} & if\ y_j(a) \leq\ U_j \\ 0 & if\ U_j <\ y_j(a) \\ 1 & if\ y_j(a) <\ y_{j\,ref} \end{cases} \tag{1}$$

and for the lower threshold L_j as:

$$M(y_j, a) = \begin{cases} \dfrac{y_j(a) - L_j}{y_{j\,ref} - L_j} & if\ L_j \leq\ y_j(a) \\ 0 & if\ y_j(a) <\ L_j \\ 1 & if\ y_j(a) >\ y_{j\,ref} \end{cases} \tag{2}$$

where $y_{j\,ref}$ is a reference value for $y_j(a)$, which can also be considered as the nominal value of the safety parameter y_j. However, a safety margin so defined ends up to be too conservatively computed not accounting explicitly for the uncertainties in the estimation of safety margin [Martorell et al., 2006; Zio et al., 2008[b]].
To overcome this conservatism, the safety margin can be defined in probabilistic terms as the difference between U_j (L_j) and the value of a specific γ_1 percentile of the distribution

of the safety parameter $y_j(a)$, accounting for both the aleatory and epistemic uncertainties that effect y. Without loss of generality, we only refer to an upper threshold U_j, the extension to L_j being straightforward. By regulation, γ_1 is usually set equal to the 95th percentile. Despite that, the estimation of the probability density function of y, $f(y)$, and of its γ-th percentile y_{γ_1}, $f(y_{\gamma_1})$, is a non-trivial task that requires guaranteeing a confidence β_1 (e.g., 95% confidence), viz [Nutt et al., 2004; Zio et al., 2010]:

$$\gamma_1 = \Pr\{y < y_{\gamma_1}\} \tag{3}$$

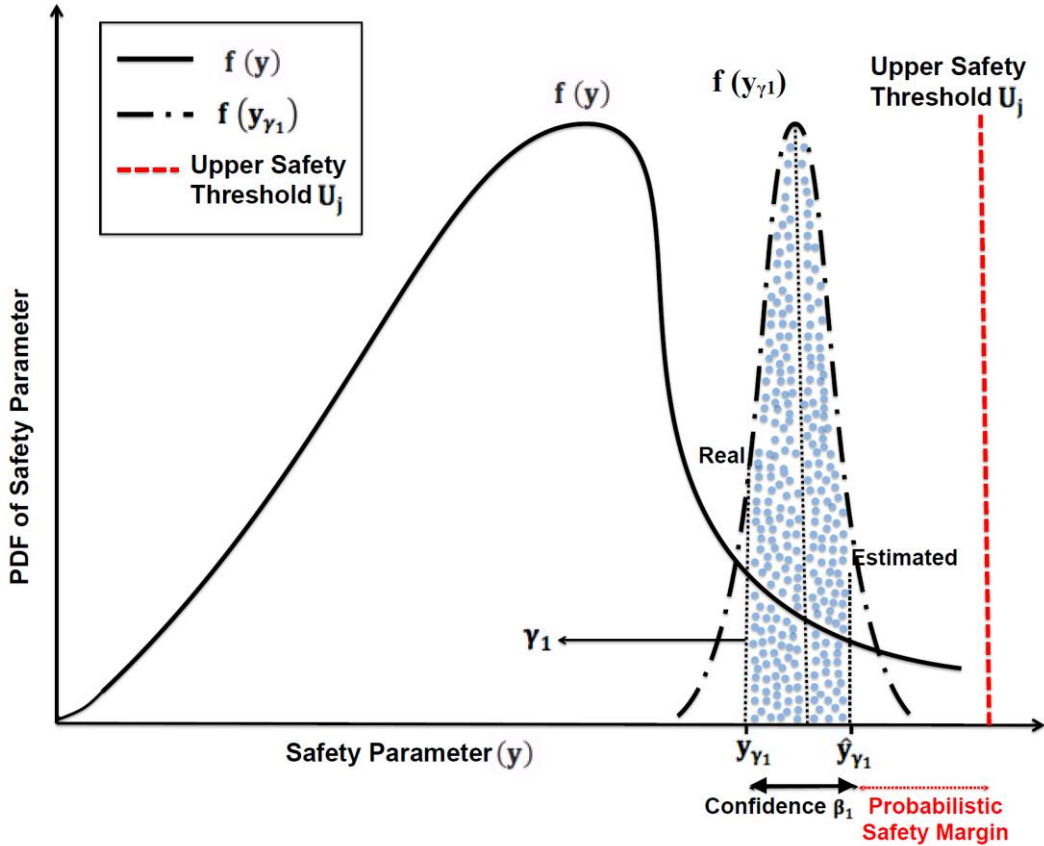$$\beta_1 = Pr\{y_{\gamma_1} < \hat{y}_{\gamma_1}\} \tag{4}$$

Figure 1 Sketch of the probability distribution of the values of safety parameter y, the probabilistic safety margin, the real y_{γ_1} and estimated $\hat{y}_{\gamma_1}$ values of a given percentile (e.g., 95th).

Figure 1 shows that $M(y_j, a) > 0$ if $y_{\gamma_1} < U_j$. Since $\hat{y}_{\gamma_1} > y_{\gamma_1}$ with confidence β_1, if $y_{\gamma_1} < U_j$, then $M(y_j, a) > 0$. After the distribution of the values of the safety parameter

y and the point estimates of the percentiles (i.e., y_{γ_1} (real) and $\hat{y}_{\gamma_1}$ (estimated)) are obtained, the probabilistic safety margin can be calculated from equation (5) [Nutt et al., 2004; Zio et al., 2008[a]]:

$$M(\gamma_1, \beta_1) = \begin{cases} \dfrac{U_j - \hat{y}_{\gamma_1}}{U_j - y_{j\,ref}} & if \ \hat{y}_{\gamma_1} \le U_j \\ 0 & if \ U_j < \hat{y}_{\gamma_1} \\ 1 & if \ \hat{y}_{\gamma_1} < y_{j\,ref} \end{cases} \tag{5}$$
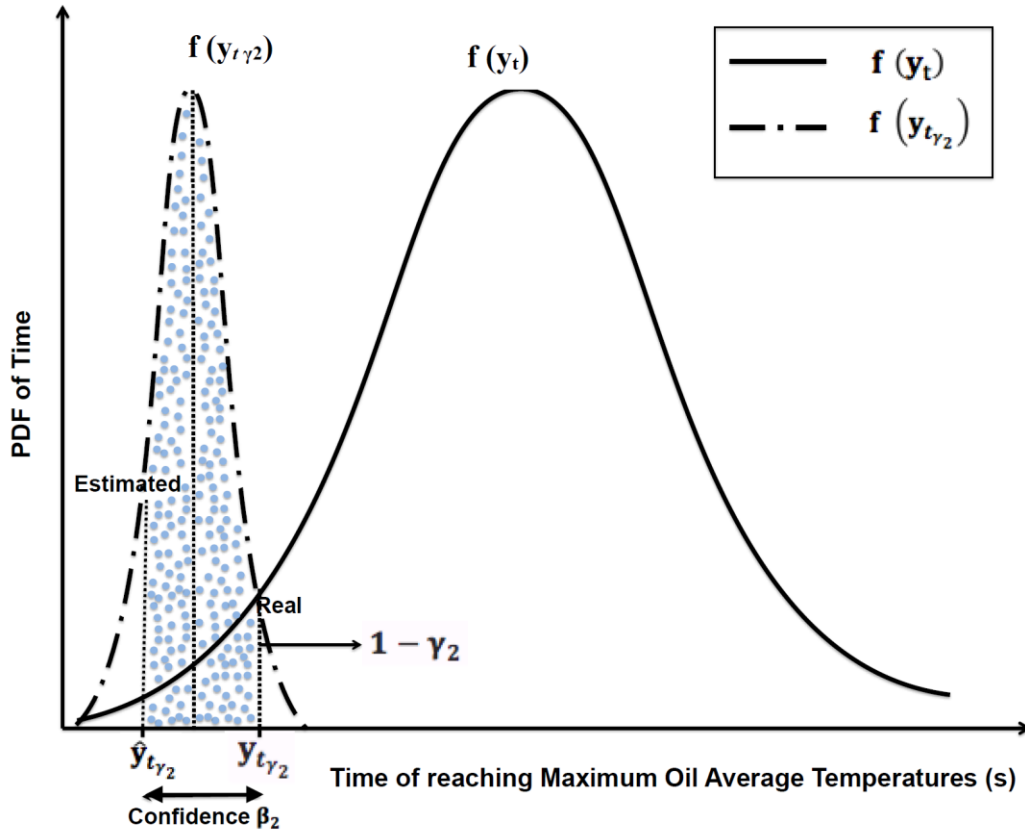

Figure 2 Sketch of the probability distribution of the values of time t, the real $y_{t_{\gamma_2}}$ and estimated $\hat{y}_{t_{\gamma_2}}$, values of a given percentile (e.g., 5th)

The definition of probabilistic safety margin of equation (5) can be enriched by taking into account the resilience information related to the time required for reaching y_{γ_1}. Similarly to y, if we consider the pdf $f(y_t)$ of time y_t required to reach y_{γ_1}, $y_{t_{\gamma_2}}$ a specific percentile (e.g., 5th percentile) of y_t and $\hat{y}_{t_{\gamma_2}}$ its estimate, then we can define (see Figure 2):

$$\gamma_2 = \Pr\left\{y_t < y_{t_{\gamma_2}}\right\} \tag{6}$$

$$\beta_2 = Pr\left\{y_{t_{\gamma_2}} > \hat{y}_{t_{\gamma_2}}\right\} \tag{7}$$

The dynamic probabilistic safety margin can, thus, be defined as a probabilistic safety margin with respect to the safety parameter y together with the information on the earliest (grace) time t required to reach that margin (i.e., the available time for counteracting the occurrence of an accidental scenario a).

$$M(\gamma_1, \gamma_2, \beta_1, \beta_2) = \left\{\begin{array}{cc} \frac{U_j - \hat{y}_{\gamma_1}}{U_j - y_{j\,ref}} & if\ \hat{y}_{\gamma_1} \le U_j \\ 0 & if\ U_j < \hat{y}_{\gamma_1} \\ 1 & if\ \hat{y}_{\gamma_1} < y_{j\,ref} \end{array}\right\} \text{ with grace time } \hat{y}_{t_{\gamma_2}} \tag{8}$$

where, the γ_2-th percentile of the grace time, $\hat{y}_{t_{\gamma 2}}$, provides the twofold information regarding: the resilience of the system not to exceed the safety threshold and the available time for undertaking counteraction measures. In other words, it provides the dynamic information for the computed probabilistic safety margin.

3. ORDER STATISTICS FOR PERCENTILES ESTIMATION

Order statistics (OS) is a non-parametric statistical quantification approach that has been shown useful in for various nuclear applications: evaluation of fuel densification [U.S. NRC, 1978], evaluation of the reliability of an Emergency Core Cooling System (ECCS) [U.S. NRC, 1996] and a Loss of Coolant Accident (LOCA) best estimate plus uncertainty nuclear safety analysis [Martin et al., 2011]. The invaluable advantage of OS is that an unlimited number of model uncertainties can be explicitly considered simultaneously, especially when the Nutt-Wallis method [Nutt et al., 2004] is enforced (as done in this work) for capturing the uncertainties in multivariate cases: this is, indeed, the only approach for multivariate cases that can determine their individual coverage with a specified confidence level and an expression of the probability distribution is not required [Martin et al., 2011].

In this study, the estimates $\hat{y}_{\gamma_1}$ and $\hat{y}_{t_{\gamma_2}}$ are quantified using OS [Nutt et al., 2004] methodology to get the optimal number of samples N of the TH code simulations to be

run to guarantee confidences β_1 and β_2 in the estimation of $\hat{y}_{\gamma_1}$ and $\hat{y}_{t_{\gamma_2}}$, respectively. This is done to avoid the computational costs for running complex TH models for obtaining the full distributions of y and y_t. [Zio et al., 2008[a]; Nutt et al., 2004]. Order Statistics and Finite Mixture Models (FMMs) [Carlos et al., 2013; Di Maio et al., 2014[b]] are used for the quantification of the uncertainties of the outputs. FMM provides a natural "clustering" of the TH code outputs, by reproducing them providing information pertaining to the most important input variables which affect the output uncertainty, whereas OS focuses on characterizing the PDFs of certain percentiles and providing approximate estimation of safety limits. This latter can also be integrated with Artificial Neural Network (ANNs) for speeding up the computation by substituting the TH code with a simpler and faster surrogate [Di Maio et al., 2015; Zio et al., 2008[b]; Mclachlan et al., 2000]. Therefore, OS allows obtaining the optimum number of samples N to be used for properly estimating the percentiles $\hat{y}_{\gamma_1}$ and $\hat{y}_{t_{\gamma_2}}$ with high confidences β_1 and β_2, respectively.

Let us assume we have a collection of two output vectors $\bar{y} = \{y_1, y_2, \ldots \ldots, y_N\}$ and $\bar{y}_t = \{y_{t_1}, y_{t_2}, \ldots \ldots, y_{t_N}\}$ that are obtained from N runs of the TH code, each one with a different input deck $\bar{x}$. Let $\bar{y}^* = \{y^{(1)}, y^{(2)}, \ldots, y^{(N)}\}$ and $\bar{y}_t^* = \{y_t^{(1)}, y_t^{(2)}, \ldots, y_t^{(N)}\}$ be the ordered set of values of the two outputs. Without loss of generality, with reference to only the safety parameter y (or the time y_t) to be limited from above by U, the approach aims at showing that the mth member y_m ($y_{t,m}$) of the N sorted output $\bar{y}^*$ ($\bar{y}_t^*$) has a certain probability β_1 (β_2) of exceeding (undershooting) the unknown true $\gamma_1 - th$ ($\gamma_2 - th$) percentile y_{γ_1} ($y_{t_{\gamma_2}}$). Then, one has a level of confidence β_1 (β_2) that the actual value of y_{γ_1} ($y_{t_{\gamma_2}}$) is less (more) than the value obtained for y_m ($y_{t,m}$): if y_m ($y_{t,m}$) meets the criterion of being less than the safety threshold U, then the unknown y_{γ_1} ($y_{t_{\gamma_2}}$) will do so, too [Nutt et al., 2004; Wald, 1943; Zio et al.,2008[a,b]]. It is worth noticing that the mth member $y_{t,m}$ of the N sorted outputs y_t is required to guarantee a confidence (β_2) of not exceeding (i.e., being smaller than) the unknown true γ_2^{th} percentile $y_{t_{\gamma_2}}$.

Two non-parametric approaches (namely Bracketing and Coverage) can be embraced to calculate N and to deal with a multi-dimensional output $\bar{y}$ and $\bar{y}_t$ and their uncertainties.

Both approaches entail two sets of outputs to be sequentially sorted. Then, from the regulatory bodies point of view, the two approaches fundamentally differ in the way they demand the outputs to satisfy their specific safety criteria. The Bracketing approach only guarantees a certain fraction of the possible nuclear safety codes outputs to be simultaneously considered, which does not guarantee adherence to all safety criteria simultaneously, but they are guaranteed to be satisfied by each output independently (or by a subset of outputs) [Nutt et al., 2004]. Coverage, on the other hand, provides a confidence that all outputs will simultaneously meet the criteria and, thus, it is expected to better conform to the regulatory conservative guidelines [Nutt et al., 2004].

3.1 Bracketing

The Bracketing approach provides the confidence that each value of the outputs from the sorted lists will be covered by the specified ranges of the cumulative probability distribution of all possible results of that output [Nutt et al., 2004]. Let γ_1 be the probability that y lies below y_{γ_1} in any of the N runs, whatever the value of y_t; γ_2 is the corresponding probability for the other output y_t. The y and y_t sets of outputs are assumed to be uncorrelated for the purpose of simplification. For uncorrelated outputs and assuming $m = 1$, we can calculate N from equation (9), where N is expressed as a function of γ and β [Nutt et al., 2004]:

$$\beta = (1 - \gamma^N)^2 \tag{9}$$

A value $N = 72$ allows calculating the $\gamma = 95^{\text{th}}$ percentile of $\bar{y}$ (i.e., $\hat{y}_{\gamma_1}$) with a $\beta = 95\%$ confidence; similarly, $\hat{y}_{t_{\gamma_2}}$ can be found by sorting $N = 72$ values of $\bar{y}_t$ [Nutt et al., 2004].

3.2 Coverage

The Coverage approach provides the confidence that each value of the sorted outputs will be covered by the specific ranges of the joint probability distribution of the outputs [Wilks, 1941; Wald, 1943; Nutt et al., 2004]. The coverage approach requires knowledge on the correlation between the outputs y and y_t. It is assumed after investigation that the sets of outputs y and y_t are found to be uncorrelated. Shortly, for uncorrelated outputs and $m = 1$, we calculate $N = 89$ resorting to equation (10) [Nutt et al., 2004]:

$$\beta = 1 - \gamma^N + N\gamma^N \ln(\gamma) \qquad (10)$$

where $\beta = 0.95$ and $\gamma = 0.95$. This value confirms that the Coverage approach requires larger number of runs as compared to the Bracketing approach. This is because in the Coverage approach (contrarily to the Bracketing approach) one output (e.g., y) is sorted jointly with the other output (e.g., y_t) and both percentiles y_{γ_1} and $y_{t_{\gamma_2}}$ are required to simultaneously lie within the estimated percentiles $\hat{y}_{\gamma_1}$ and $\hat{y}_{t_{\gamma_2}}$ to guarantee the confidence β_1 and β_2.

4. THE LBE-XADS SYSTEM

The Lead-Bismuth Eutectic eXperimental Accelerator Driven System (LBE-XADS) is a sub-critical, fast reactor in which the fission process for providing thermal power $P(t)$ is sustained by an external neutron source through spallation reaction by a proton beam $Q(t)$ accelerated by a synchrotron on a lead-bismuth eutectic target: a simple scheme of the system is given in Figure 3 [Cammi et al., 2006].

The primary cooling system is of pool-type with Lead-Bismuth Eutectic (LBE) liquid metal coolant leaving the top of the core, at full power nominal conditions, at temperature $\tau_{LB}^{C,P}$ equal to 400 [°C] pushed by natural circulation enhanced by argon gas injection into the heat exchangers of the secondary cooling circuit and then re-entering the core from the bottom through the down-comer at temperature $\tau_{LB}^{P,C}$ equal to 300 [°C]. The average in-core temperature of the LBE $T_{LB}^{av,C}$ is taken as the mean of $\tau_{LB}^{C,P}$ and $\tau_{LB}^{P,C}$ [Di Maio et al., 2009]. The secondary cooling system is a flow of diathermic oil at 290-320 [°C], at full power conditions. Cooling of the diathermic oil is obtained through an airflow $\Gamma_a(t)$ provided by three air coolers connected in series [Di Maio et al., 2009].
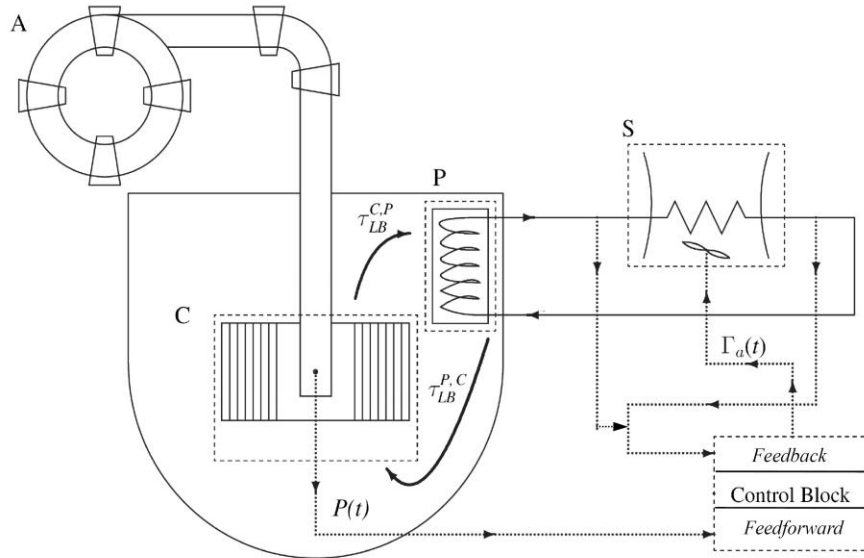
Figure 3 LBE-XADS simplified schematics. A = Accelerator; C = core; P = primary heat exchanger; S = secondary heat exchanger [Cammi et al., 2006]

A dedicated, dynamic simulation model, as shown by a block diagram in Figure 4, has been implemented in SIMULINK for providing a simplified, lumped and zero-dimensional description of the coupled neutronic and thermo-hydraulic evolution of the system [Cammi et al., 2006]. The interested reader may refer to [Cammi et al., 2006] for further details of the model considered. The control system aims to keep the average oil temperature value approximately around 300 [°C] (573.15 [K]), which is the optimum working temperature of the diathermic oil under steady state, nominal condition at full power 80 [MW_{Th}].
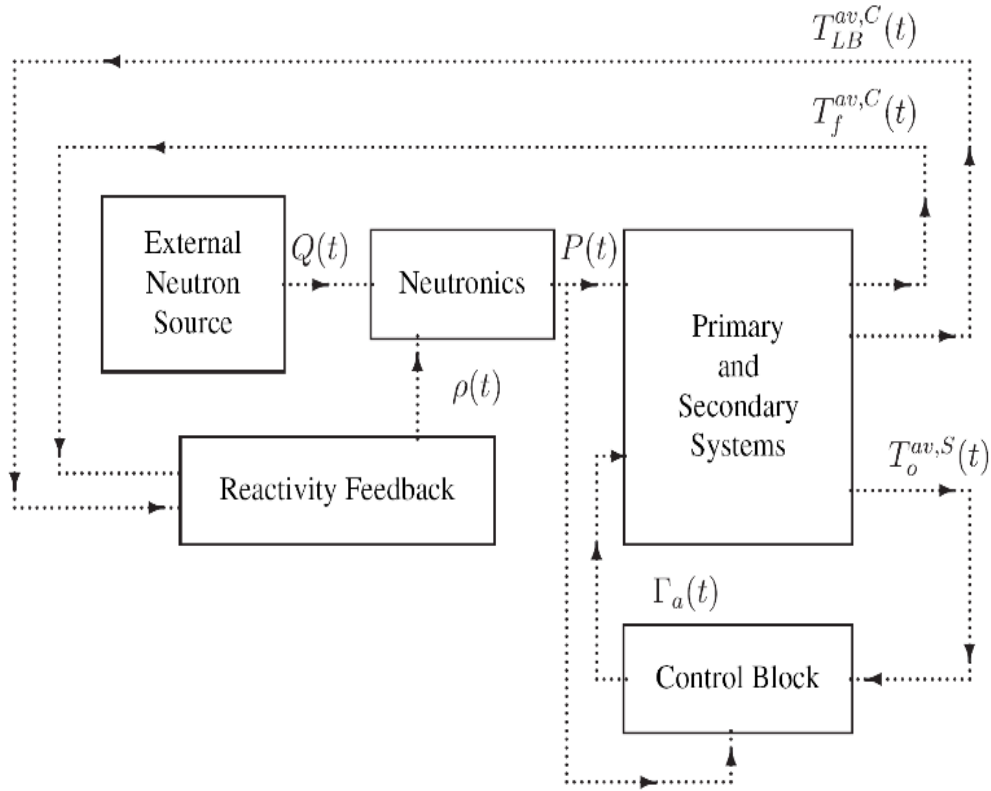
13

Figure 4 Block diagram representing the SIMULINK model of the LBE-XADS [Cammi et al., 2006]

As described in [Cammi et al., 2006], the upper safety threshold $T_o^{th,u}$ considered is 340 [°C] (613.15 [K]) beyond which the changes in the physical and chemical properties of the oil will render it inefficient while a temperature below a lower safety threshold $T_o^{th,l}$ of 260 [°C] (533.15 [K]) can result in thermal shocks of the primary fluid and thus the structural components. The controlled variable is the average temperature of diathermic oil ($T_o^{av,S}$), whereas the control variable is the mass flow rate of air (Γ_a) in the air coolers battery. In Figure 5, the profile of the average temperature of diathermic oil ($T_o^{av,S}$) at full power nominal conditions (i.e., without component failures and with input parameter equal to the mean values listed in Table 1) is shown: even if the system is stable at nominal conditions (303.85 [°C] or 577 [K]), the discrete-state regulation of the air coolers causes visible ripples of the diathermic oil temperature [Di Maio et al., 2009].
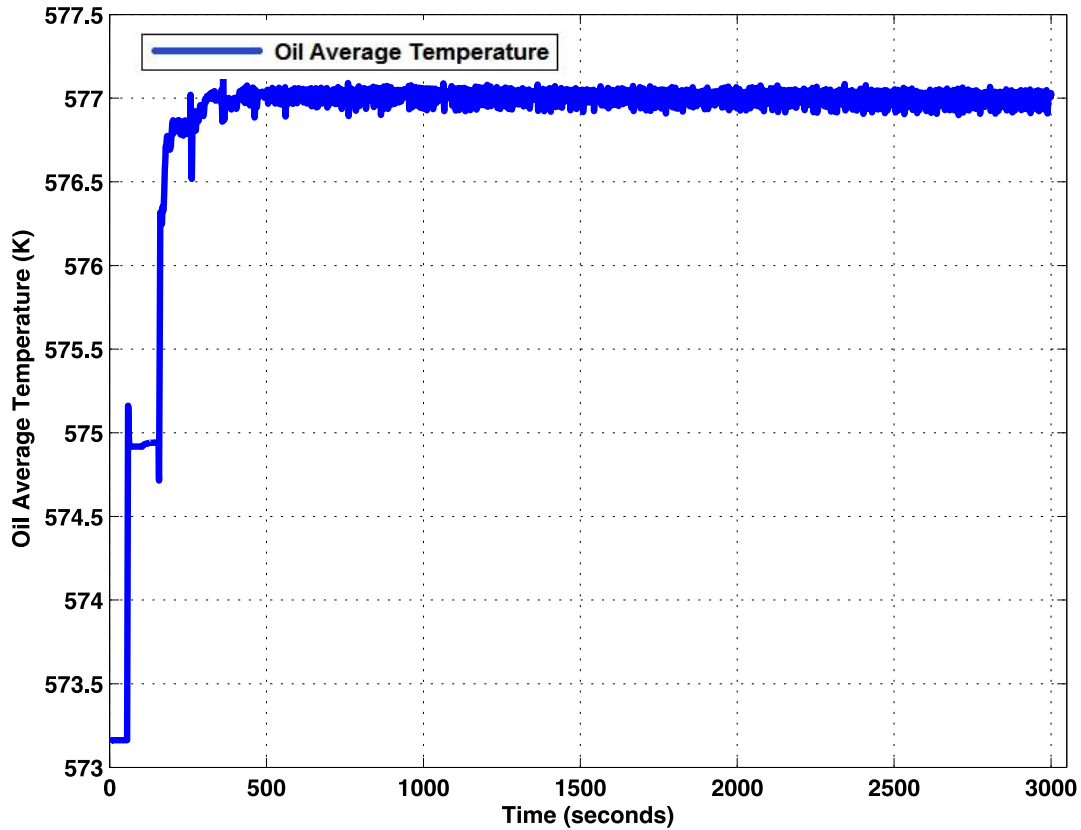
Figure 5 Oil average temperature evolution at nominal conditions

4.1 The Monte- Carlo Driven Fault Injection Engine

In order to simulate transients representative of the dynamic failure behavior of the LBE-XADS, the SIMULINK model has been embedded within a MC procedure for sampling the values of the input physical variables from their respective uncertainty distributions (epistemic uncertainty) and injecting faults at random times and of random magnitudes (aleatory uncertainty).

4.1.1. Epistemic Uncertainty

The physical input parameters that are fed to the SIMULINK model have been randomly sampled from their respective distributions as given in Table 1, where the chosen distributions have been taken from the listed references.

15

Parameter	Range of parameter distribution		Mean μ	Standard Deviation σ	Probability distribution
	Min	Max			
$\beta_{delayed}$ (Fraction of delayed neutrons) [%] [Cammi et al., 2006]	0.0033	0.0037	0.0035	6.42E-05	Normal
C_a (Air Specific heat capacity) [kJ/kg-K] [Panasiti et al., 1999]	0.973	1.027	0.999	0.0089	Normal
C_f (Fuel specific heat capacity) [kJ/kg-K] [ORNL, 2000]	0.234	0.265	0.250	0.0052	Normal
$Gamma_{a0}$ (Initial air mass flow rate) [kg/s] [Agostini et al., 2005]	694.11	910.85	802.48	36.12	Normal
$Gamma_o$ (Oil Mass Flow rate) [kg/s] [Agostini et al., 2005]	699.60	965.50	832.55	44.32	Normal
$Gamma_p$ (Lead Mass Flow rate) [kg/s] [Agostini et al., 2005]	4630.54	6254.78	5442.66	270.71	Normal
M_a (Mass of air) [kg] [Cammi et al., 2006]	139.79	185.18	162.48	7.56	Normal
Mf (Mass of fuel) [kg] [Cammi et al., 2006]	3540.14	3750.65	3645.39	35.09	Normal
Mo_1 (Mass of oil in Loop 1) [kg] [Cammi et al., 2006]	1505.12	2008.12	1756.62	83.83	Normal
Mo_2 (Mass of oil in Loop 2) [kg] [Cammi et al., 2006]	3651.55	4780.99	4216.27	188.24	Normal
Mp_1 (Mass of lead in Loop 1) [kg] [Anderson et al., 1986]	9469.96	13673.72	11571.84	700.63	Normal
Mp_2 (Mass of lead in Loop 2) [kg] [Anderson et al., 1986]	56160.75	82239.52	69200.13	4346.46	Normal
Tf_{ave_0} (Average initial temperature of fuel) [K] [D' Angelo et al., 2003]	972.36	1162.90	1067.63	31.76	Normal
Tp_{in_0} (LBE temperature entering Primary HX- Core Loop) [K] [NEA, OECD, 2011]	530.15	617.49	573.82	14.56	Normal
Tp_{out_0} (LBE temperature leaving Primary HX-Core Loop) [K] [NEA, OECD, 2011]	623.79	727.85	675.82	17.34	Normal
Q (Source value) [Negrini et al., 2003]	0.0943	0.1061	0.1002	0.002	Normal
P_o (Total thermal power of XADS in steady state) [kWth](assumed)	80000	82682.42	80000	-	Uniform
K (Multiplication factor, nominal power, BOC) [Negrini et al., 2003]	0.95	0.99	0.97	-	Uniform
Ta_{in} [Air inlet temperature from air coolers) [K]	281.48	318.02	299.75	6.09	Seasonal

Table 1 Distributions of physical parameters

The result of the random sampling of the physical parameters fed to the SIMULINK model of the LBE- XADS is given in Figure 6 where a large set of transients are plotted whose evolution is affected by the sampled values of input parameters. The randomness of the evolution of the oil average temperature ($T_o^{av,S}$) in comparison with its nominal case (shown in Figure 5) is due to the inherent variability and combination of the sampled physical variables. Nevertheless, the inherent uncertainties of the physical variables do

not lead the system to failure (none of the transients exceeds the upper and lower thresholds at 340 °C (613.15 K) and 260 °C (533.15 K), respectively).
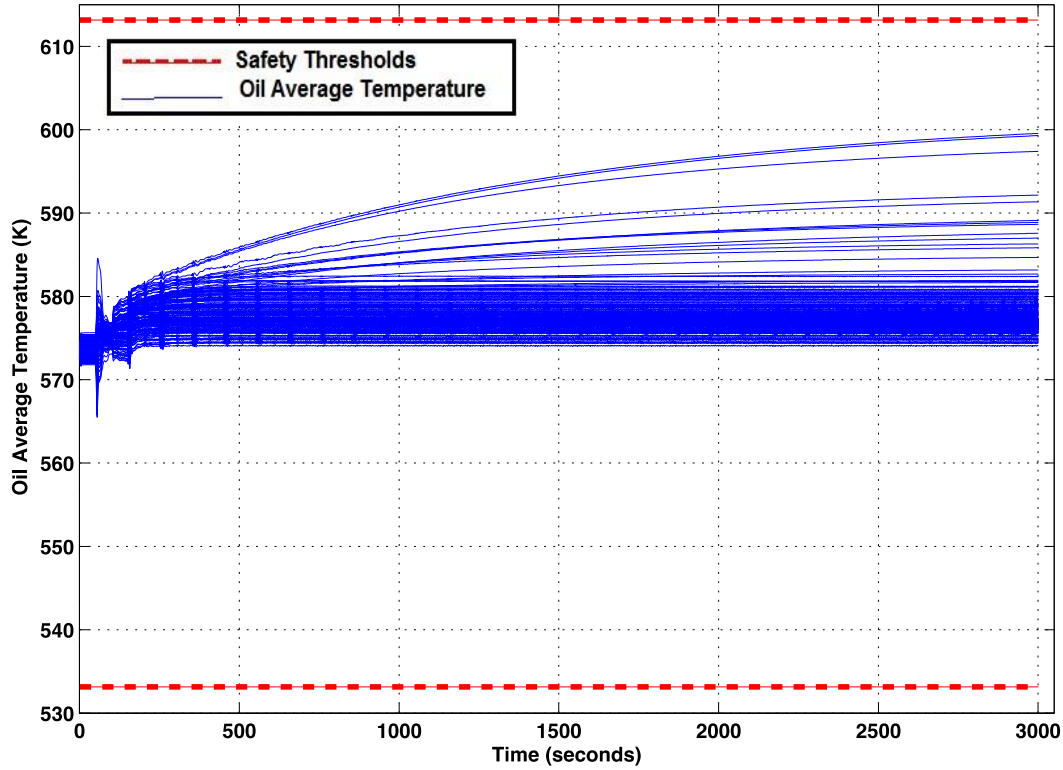

Figure 6 Oil Average Temperature with physical variables uncertainties and no initiating events

4.1.2. MC fault injection

The dynamics of the failures of the LBE-XADS system are explained focusing on four faults, as shown in Figure 7, which are:

- The PID controller fails stuck with a random flow rate output value m_1 sampled from a uniform distribution in [0,797] [kg/s].

- The air coolers fail stuck in a random position that provides a corresponding air flow mass m_2 uniformly distributed in [0,1000] [kg/s].

- The feedforward controller fails stuck with a corresponding flow rate value m_3 uniformly distributed in [0,797] [kg/s].

- The communication between air coolers actuators and PID controller fails so that the PID is provided with the same input value of the previous time step.

17

The choice of a mission time T_M of 3000 [s] has been made, because it is a long enough interval of time to allow the complete development also of slow dynamic accident scenarios occurring at early/medium times [Di Maio et al., 2009].
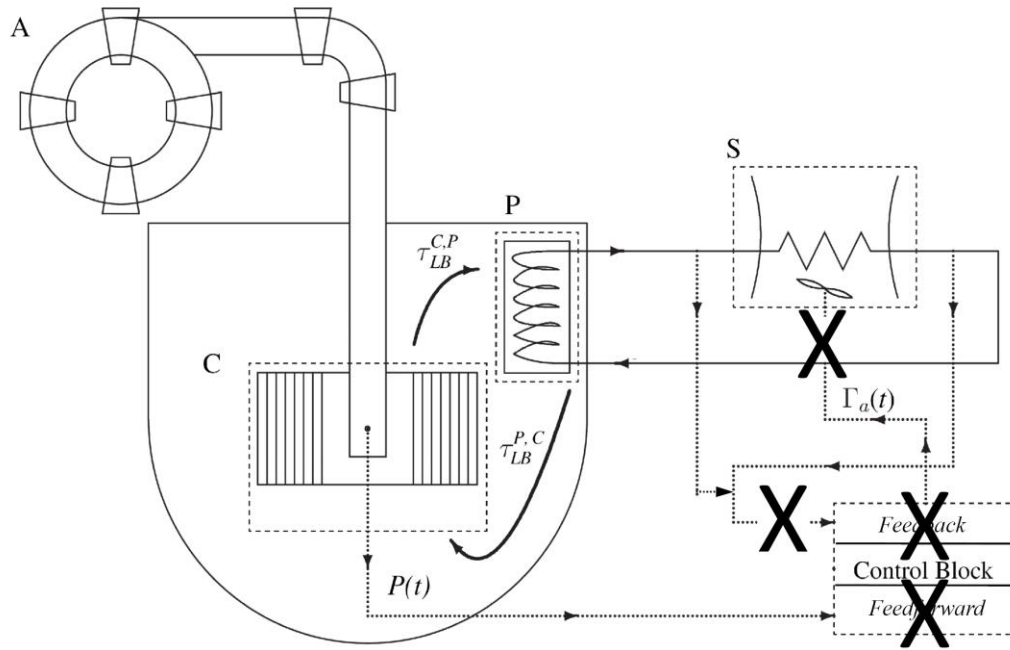

Figure 7 Sketch of the faults that can be injected into the system: the PID controller fails stuck at a random output value, the air coolers fails stuck at a random position, the feedforward control fails stuck a random output value, the communication between air coolers actuators and the PID controller is interrupted

Within the mission time T_M of 3000 s, the transients can lead to three end states:

1. Low-temperature failure mode $(T_o^{av,S} < T_o^{th,l})$
2. Safe mode $(T_o^{th,l} < T_o^{av,S} < T_o^{th,u})$
3. High-temperature failure mode $(T_o^{av,S} > T_o^{th,u})$

A comprehensive quantitative reliability assessment of the system is expected to involve all system components and failure modes and the dynamic effects arising from the complex interactions of all system elements, including the software and the human (here not modeled) [Di Maio et al., 2009]. However, to reduce the computational burden and to avoid the complexity of combinatorial explosion of a DET in such situation [Di Maio, 2009], we consider the ad-hoc case study hereafter described and sketched in Figure 8.

As an example of a dynamic evolution of an accidental scenario among the infinite number of scenarios that might be considered in a DET for IDPSA, we limit our analysis to those scenarios leading to high-temperature failure mode (the upper safety threshold is equal to $U_j = T_o^{th,u} = 613.15$ [K]) and, among these, to the scenarios that consist in multiple successive failures of the air coolers getting stuck at random times and magnitudes (whose distributions are given in Table 2).

	Air Mass Flow [kg/s]		Time [s]		Probability distribution
	Min	Max	Min	Max	
Air Cooler fails stuck (First failure)	630	645	600	800	Uniform
Air Cooler fails stuck (Second failure)	850	850	1000	1200	Uniform

Table 2 Uncertainty distributions of failure time and magnitude for the DET scenario considered.

The set of failure events that occur during this accidental scenario are not Prime Implicants (PIs) (i.e., these are not the minimum combination of failure events, with certain order and timing, that could lead the system to failure) [Di Maio et al., 2015; Garret et al., 1999]). Thus, this set of failure events does not unequivocally determine the end-state of the system as a failure, but, rather, it is a 'near-miss' scenario [Di Maio et al., 2009]. These failure events make the temperature $T_o^{av,S}$ approach the upper safety threshold $T_o^{th,u}$ without exceeding it, as shown in Figure 9, where the evolution of 104 safe transients of $T_o^{av,S}$ towards $T_o^{th,u}$ are plotted, when the selected accidental scenario of Table 2 (and sketched in bold line in Figure 8) is injected into the SIMULINK model of the LBE-XADS along with the uncertainties of its physical variables (as given in Table 1).
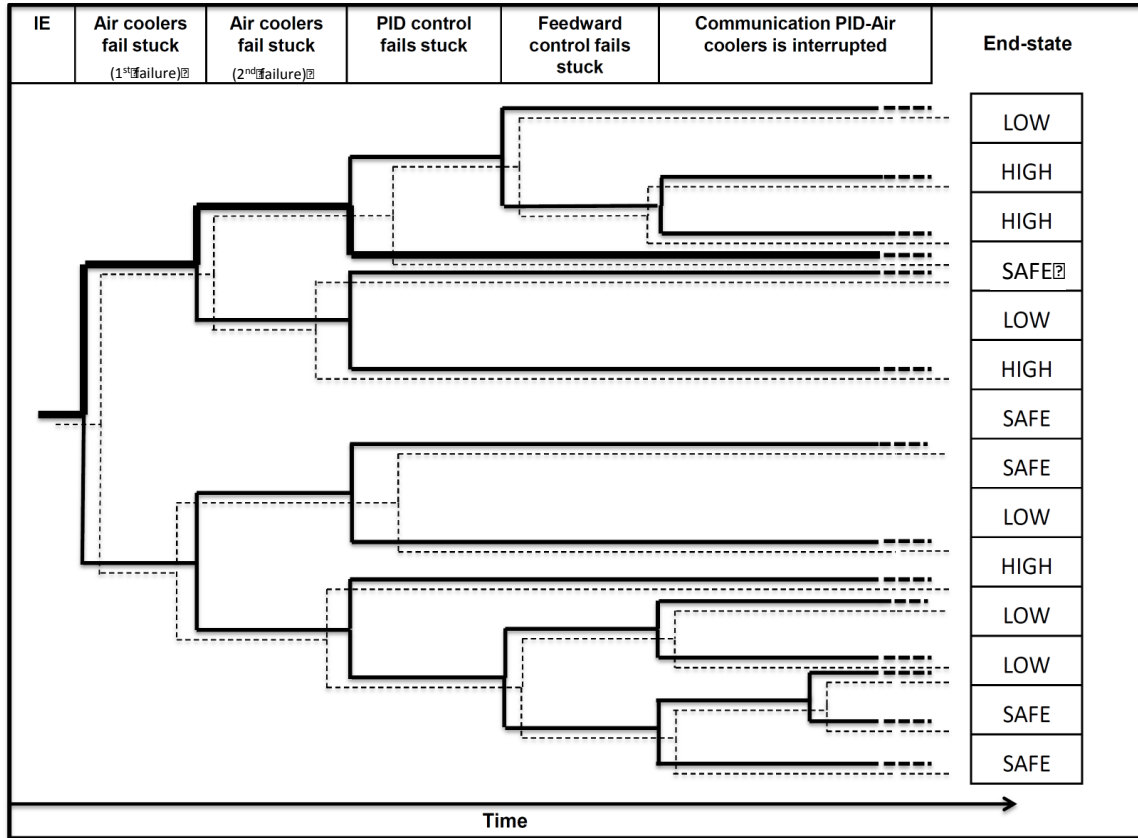
IE	Air coolers fail stuck (1st failure)	Air coolers fail stuck (2nd failure)	PID control fails stuck	Feedward control fails stuck	Communication PID-Air coolers is interrupted	End-state

End-states (top to bottom): LOW, HIGH, HIGH, SAFE, LOW, HIGH, SAFE, SAFE, LOW, HIGH, LOW, LOW, SAFE, SAFE

Time

Figure 8. A conceptual sketch of a DET. The bold line indicates one of the infinite sequences that can take place.

It is worth pointing out that the random timings and magnitudes of successive failures cause randomness in the system dynamics (as shown in Table 3, where, the maximum temperature reached $T_{o,max}$ and the time y_t at which this is reached are listed for each transient that is plotted in Figure 9). The need of assessing the risk related to the occurrence of this scenario, in terms of both the capability of the system to keep $T_o^{av,S}$ below $T_o^{th,U}$ and the availability of time for counteracting the temperature rise, calls for the quantification of a DSM.

To do this, we aim at estimating, with a given confidence β, the 95th percentiles of the distribution of $T_{o,max}$ and the 5th percentile of the distribution of the time required to reach these temperatures.
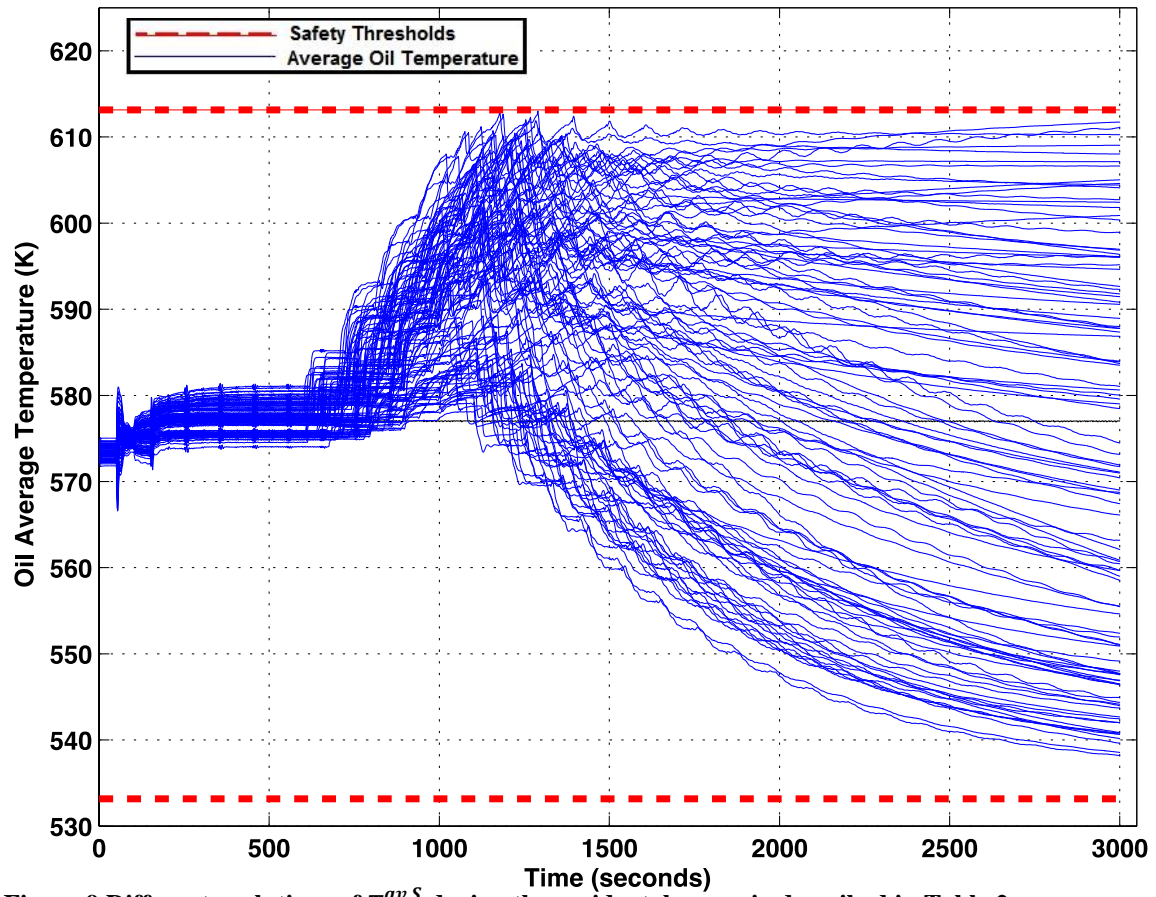
Figure 9 Different evolutions of $T_o^{av,S}$ during the accidental scenario described in Table 2

Simulation#	$T_{o,max}$	Time y_t (s)	Simulation#	$T_{o,max}$	Time y_t (s)
1	586.20	1088	53	593.63	1142
2	600.16	1114	54	608.09	1295
3	579.50	1079	55	604.14	1199
4	603.24	1110	56	605.03	3001
5	594.18	1133	57	599.73	1222
6	600.06	1232	58	584.17	1109
7	584.67	1049	59	581.69	1139
8	594.03	1189	60	581.56	1194
9	595.27	1157	61	593.31	1128
10	604.31	1223	62	612.64	1188
11	603.64	1282	63	601.61	1243
12	596.68	1112	64	600.87	3001
13	608.01	1234	65	602.65	1123
14	582.46	1021	66	597.07	1263
15	610.94	1251	67	608.83	1209
16	580.56	1105	68	596.54	1170
17	588.56	1064	69	585.51	1110
18	595.52	1191	70	611.99	1255
19	611.12	3001	71	611.19	1123
20	601.19	1278	72	584.12	1156
21	593.56	1251	73	610.45	1222
22	598.68	1124	74	596.84	1181
23	588.28	1158	75	580.99	1001
24	609.73	1211	76	588.67	1097

25	602.28	1236	77	599.92	1141
26	604.02	1175	78	584.95	1108
27	578.59	1125	79	589.57	1151
28	600.18	1246	80	595.41	1156
29	606.33	1248	81	594.57	1134
30	599.17	1170	82	600.09	1139
31	609.03	1257	83	587.14	1031
32	612.29	1268	84	610.74	1158
33	609.55	1241	85	603.36	1231
34	604.61	3001	86	601.64	1221
35	605.51	1161	87	583.25	1131
36	599.60	1124	88	599.56	1088
37	610.17	1299	89	604.99	1232
38	606.63	1260	90	584.69	1141
39	584.01	1060	91	583.97	1117
40	580.54	1132	92	597.29	1188
41	589.23	1129	93	608.01	1198
42	602.08	1295	94	612.93	1178
43	598.52	1103	95	611.74	3001
44	607.58	1268	96	582.39	1049
45	608.32	1209	97	584.82	1163
46	603.48	1166	98	581.19	1180
47	594.41	1178	99	589.34	1172
48	603.91	1255	100	586.66	1109
49	580.10	1101	101	591.04	1121
50	581.33	1051	102	586.97	1197
51	612.99	1290	103	586.82	1157
52	583.84	1085	104	582.68	1049

Table 3 List of the maximum value of the average oil temperature that is reached in the simulations of Figure 9 and the respective times.

4.2 Results and Discussions

For applying the Bracketing and Coverage approaches to $y = T_{o,max}$ and y_t, $N = 72$ and $N = 89$ samples are randomly selected from the 104 safe transients plotted in Figure 9 and listed in Table 3. In both cases, m has been chosen to be equal to 1, γ_1 equal to 0.95, γ_2 equal to 0.05 and β_1 and β_2 equal to 95%. In practice, we want to quantify the dynamic probabilistic safety margin for the selected accidental scenario by quantifying a reasonable grace time $\hat{y}_{t_{\gamma_2}}$ before the estimated temperature $\hat{y}_{\gamma_1}$ is reached. Indeed, the value of $\gamma_2 = 5^{th}$ percentile with $\beta_2 = 95\%$ will allow the operator to know the time at his disposal with large confidence for mitigating the risk of the onset of the selected accidental scenario.

4.2.1 Results using Bracketing approach

Using the $N = 72$ samples, the results of the point estimates of the 95th percentile (γ_1) of Maximum Oil Temperature and the 5th percentile (γ_2) of the time taken to reach the

22

maximum temperature, as computed by the Bracketing OS method on the sample $\bar{y} = \{y_1, y_2, \ldots\ldots, y_N\}$ and $\bar{y}_t = \{y_{t_1}, y_{t_2}, \ldots\ldots, y_{t_N}\}$ are given in Table 4. <mark>The two sets of outputs $\bar{y}$ and $\bar{y}_t$ are independently sorted in descending and ascending order, respectively. The $m-$th value of the sorted $\bar{y}$ of the $N = 72$ $T_{o,max}$ values sampled from Table 3 is assumed (according to OS theory) to exceed the real 95th percentile of $\bar{y}$ with a probability of 95%. Similarly for $\bar{y}_t$, the $m-$th value is considered to be that time which with probability 95% underestimate the 5th percentile of $\bar{y}_t$.</mark>

Safety parameter y (maximum oil temperature $T_{o,max}$ [K])					
Estimated 95th percentile value, $\hat{y}_{\gamma_1}$	Real 95th percentile value, y_{γ_1}	Upper safety threshold U	Nominal value, y_{ref}	DSM	Distribution
612.99	611.89	613.15	577.12	0.0044	Weibull
Distribution of time [s] to reach $T_{o,max}$					
Estimated 5th percentile value $\hat{y}_{t_{\gamma_2}}$		Real 5th percentile value $y_{t_{\gamma_2}}$		Distribution	
1088		1102.56		Normal	

Table 4 Point estimates of the percentiles of the $T_{o,max}$ and the time to reach the maximum temperature with the Bracketing approach

The DSM for the safety parameter y is calculated using equation (8), where the reference value y_{ref} is taken equal to 577.12 [K]. The real y_{γ_1} is calculated as the γ_1^{th} percentile (95th) of the distribution of $\bar{y}$, that turns out to be a Weibull distribution by Anderson-Darling (AD) statistical hypothesis test [Ali, 2012]. <mark>The Weibull probability distribution of the $T_{o,max}$ has a y_{γ_1} equal to 611.89 [K], which is smaller than $\hat{y}_{\gamma_1} = 612.99$ [K] and, thus, also smaller than $U = 613.15$ [K].</mark> The real $y_{t_{\gamma_2}}$ is calculated as the γ_2^{th} percentile (5th) of the distribution $\bar{y}_t$ that turns out to be a Normal distribution, identified using AD statistical hypothesis test [Jäntschi and Bolboacã, 2009].

<mark>Thus, the Normal distribution of $\bar{y}_t$ at which $T_{o,max}$ is reached has the value $y_{t_{\gamma_2}} = 1102.56$ [s], which is larger than the $\hat{y}_{t_{\gamma_2}} = 1088$ [s].</mark>

4.2.2. Results using Coverage approach

The same analysis is done using the Coverage approach on $N = 89$ selected samples. The outcomes of the point estimates of the 95th percentile (γ_1) of $T_{o,max}$ and the 5th percentile (γ_2) of the time taken to reach the maximum temperature, as computed by the Coverage OS method on the sample $\bar{y} = \{y_1, y_2, \ldots \ldots, y_N\}$ and $\bar{y}_t = \{y_{t_1}, y_{t_2}, \ldots \ldots, y_{t_N}\}$, are given in Table 5. The two sets of outputs $\bar{y}$ and $\bar{y}_t$ are jointly sorted in descending order for the $\bar{y}$ set of values and its corresponding time from the $\bar{y}_t$ set as given in Table 3. The $m-$th value of the sorted $\bar{y}$ of the $N = 89$ $T_{o,max}$ values samples from Table 3 is assumed (according to OS theory) to exceed the real 95th percentile of $\bar{y}$ with a probability of 95% while also, simultaneously for $\bar{y}_t$, the $m-$th value of the sorted $\bar{y}_t$ is considered to be that time which with a probability of 95% underestimates the 5th percentile of $\bar{y}_t$.

The DSM for the safety parameter y is again calculated using equation (8), where the reference value y_{ref} is taken equal to 577.12 [K] and the real y_{γ_1} is calculated as the γ_1^{th} percentile (95th) of the distribution of $\bar{y}$ that turns out again to be a Weibull distribution by Anderson-Darling (AD) statistical hypothesis test [Ali, 2012]. The Weibull probability distribution of the $T_{o,max}$ has a y_{γ_1} equal to 611.76 [K] which is smaller than $\hat{y}_{\gamma_1} = 612.99$ [K] and, thus, also smaller than $U = 613.15$ [K]. The real $y_{t_{\gamma_2}}$ is calculated as the γ_2^{th} percentile (5th) of the distribution of $\bar{y}_t$ that turns out to be a Gamma distribution by the AD statistical hypothesis test [Won, 1996].

Safety parameter y (maximum oil temperature $T_{o,max}$ [K])					
Estimated 95th percentile value, $\hat{y}_{\gamma_1}$	Real 95th percentile value, y_{γ_1}	Upper safety threshold U	Nominal value, y_{ref}	DSM	Distribution
612.99	611.76	613.15	577.12	0.0044	Weibull
Distribution of time [s] to reach $T_{o,max}$					
Estimated 5th percentile value $\hat{y}_{t_{\gamma_2}}$		Real 5th percentile value $y_{t_{\gamma_2}}$		Distribution	
1031		1076		Gamma	

Table 5 Point estimates of the percentiles of the $T_{o,max}$ and the time to reach the maximum temperature with the Coverage approach

Thus, the Gamma distribution of $\bar{y}_t$ at which $T_{o,max}$ is reached has the value $y_{t_{\gamma_2}} = 1076$ [s], which is larger than the $\hat{y}_{t_{\gamma_2}} = 1031$ [s].

It is to be observed that the point estimates of the 95th percentile and the 5th percentile (as shown in Table 4 and Table 5, respectively) guarantee the dynamic probabilistic safety margin to be positive in both cases of Bracketing and Coverage, and provide additional integrated information about the grace time before $T_{o,max}$ is reached.

As a concluding remark, it is worth noticing that both the dynamic probabilistic safety margins of Tables 4 and 5 result to be equal to 0.0044 with Bracketing and Coverage approaches, respectively. This is not surprising, because these results have been obtained with a different number N of simulations. The Coverage approach is more computationally burdensome ($N = 89$ samples required) as compared to the Bracketing approach ($N = 72$ samples required). This is because the Bracketing approach provides a safety margin when both outputs ($T_o^{av,S}$ and t) are tested to independently meet the safety criteria, while the Coverage approach guarantees for both outputs to simultaneously fall into the acceptable criteria.

5. CONCLUSION

In this work, we address the problem of the estimation of dynamic probabilistic safety margin for taking into account the aleatory and epistemic uncertainties affecting the physical behavior of dynamic systems. We adopt by using Order Statistics and Finite Mixture Models approaches to jointly estimate percentiles of the distributions of the safety parameter and of the time required for the safety parameter to reach these percentiles values. This information, here originally provided within the framework of safety margin, is quite important in practice.

The computational framework has been developed with respect to an accidental sequence considered in an IDPSA that might occur in the LBE-XADS system. The result of the OS approaches of Bracketing and Coverage for the LBE-XADS case study confirms the capability of the proposed framework for the quantification of the safety margin and the estimation of the grace time with a given confidence. Using an optimal number of samples N as proposed by the OS theory, the point estimates of the percentiles of the

distributions of a safety parameter and of the earliest time required for the safety parameter to reach this percentile can be computed for estimating the dynamic probabilistic safety margins with a given confidence.

ACKNOWLEDGEMENT

REFERENCES

[Agostini et al., 2005] Agostini, P., Alemberti, A., Ambrosini, W., Benamati, G., Bertacci, G., Cinotti, L., Elmi, N., Forgione, N., Oriolo, F., Scaddozzo, G., Tarantino, M. Testing and Qualification of Circe Venturi-Nozzle Flow Meter for Large Scale Experiments. 13th International Conference on Nuclear Engineering, Beijing, China, May 16-20, 2005, ICONE 13-50909, (2005).

[Aldemir, 2013] Aldemir, T. A survey of dynamic methodologies for probabilistic safety assessment of nuclear power plants. Annals of Nuclear Energy, Vol. 52, pp. 113-124, (2013).

[Ali, 2012] Ali, R.A.H. fitting a Two Parameters of Weibull Distribution Using Goodness of Fit tests. Al- Mustansiriyah J. Sci., Vol. 23, No. 6, (2012).

[Anderson et al., 1986] Anderson, J.L., Anderson, R.L., Morelock, T.C. (Oak Ridge National Laboratory), Hauang, T.L., Phillips, L.E. (U.S. Nuclear Regulatory Commission). Instrument Accuracy in Reactor Vessel Inventory Tracking Systems. Martin Marietta Energy systems, Inc., (1986).

[Apostolakis, 1990] Apostolakis, G.E. The Concept of Probability in Safety Assessments of Technological Systems. Science, Vol. 250, No. 4986, pp. 1359-1364, (1990).

[Carlos et al. 2013] S. Carlos, A. Sánchez, D. Ginestar, S. Martorell. Using finite mixture models in thermal-hydraulics system code uncertainty analysis. Nuclear Engineering and Design, Volume 262, September 2013, Pages 306-318, (2013).

[Cammi et al., 2006] Cammi, A., Luzzi, L., Porta, A. A., Ricotti, M. E. Modelling and control strategy of the Italian LBE-XADS, Progress in Nuclear Energy, Volume 48, Issue 6, Pages 578-589, (2006).

[D' Angelo et al., 2003] D'Angelo, A, Gabrielli, F. Benchmark on Beam Interruptions in an Accelerator-driven System. Nuclear Science, ISBN 92-64-02138-8, NEA/NSC/DOC(2003)17, Nuclear Energy Agency, OECD, (2003).

[Devooght, 1997] Devooght, J. Dynamic Reliability. Advances in Nuclear Science and Technology, Vol. 25, pp. 215-278, (1997).

[Di Maio et al., 2009] Di Maio, F., Zio, E. Processing dynamic scenarios from a reliability analysis of a nuclear power plant digital instrumentation and control system. Annals of Nuclear Energy 36 (2009) 1386–1399, pp. 1386-1396, (2009).

[Di Maio et al., 2014ª] F. Di Maio, G. Nicola, E. Zio, Y.Yu, "Ensemble-based sensitivity analysis of a best estimate thermal hydraulic model: application to a Passive Containment Cooling System of an AP1000 Nuclear Power Plant", Annals of Nuclear Energy, 73, 200–210, 2014

[Di Maio et al.2014ᵇ] Di Maio, F., Nicola, G., Zio, E., Yu, Y. Finite Mixture Models for Sensitivity Analysis of Thermal Hydraulics codes for Passive Safety Systems analysis. Nuclear Engineering and Design, 289, 144–154, (2014).

[Di Maio et al.2015] Di Maio, F., Baronchelli, S., Zio, E. A Computational Framework for Prime Implicants Identification in Noncoherent Dynamic Systems. Society for Risk Analysis, doi: 10.1111/risa.12251, Vol. 35, No. 1, 142–156, (2015).

[Dufour and Dutuit, 2002] Dufour, F. and Dutuit, Y., 2002. Dynamic reliability: A new model. 13th ESREL2002 European Conference, Lyon-France, pp. 18–21, (2002).

[Garret et al., 1999] Garret C. J., Apostolakis G.E. Context in the risk assessment of digital systems. Risk Analysis, Volume 19, Issue 1, Pages 23-32, (1999).

[Helton, 2011] Helton, J.C. Quantification of Margins and Uncertainties: Conceptual and Computational Basis. Reliability Engineering and System Safety, Vol. 96, pp. 976–1013, (2011).

[IAEA SSG-2, 2009] International Atomic Energy Agency. Deterministic Safety Analysis for Nuclear Power Plants, Safety Standards Series No. SSG-2, (2009).

[Jäntschi and Bolboacã, 2009] Jäntschi, L., & Bolboacã, S.D. Distribution fitting 2. Pearson-Fisher, Kolmogorov-Smirnov, Anderson-Darling, Wilks-Shapiro, Cramser-von-Misses and Jarque-Bera statistics, (2009).

[Labeau et al., 2000] Labeau, P.E., Smidts, C., Swaminthan, S. Dynamic Reliability: Towards an Integrated Platform for Probabilistic Risk Assessment. Reliability Engineering and System Safety, Vol. 68, Issue 3, pp. 219-254, (2000).

[Marseguerra et al., 1998] Marseguerra, M., Zio,E., Devooght, J., Labeau, P.E. A concept paper on dynamic reliability via Monte Carlo simulation, Mathematics and Computers in Simulation, Volume 47, Issues 2–5, 1 August 1998, Pages 371–382, (1998).

[Martin et al., 2011] Martin, R.P., Nutt, W.T. Perspectives on the application of order-statistics in best-estimate plus uncertainty nuclear safety analysis. Nuclear Engineering and Design 241, pp. 274-284, (2011).

[Martorell et al., 2006] Martorell, S., Nebot, Y., Villanueva, J.F., Carlos, S., Serradell, V., Pelayo, F., Mendizàbal, R. Safety Margins Estimation Method Considering Uncertainties within Risk-Informed Decision Making Framework. In "*Proceedings of the PHYSOR 2006 Conference*", Vancouver, Canada, September 10-14, (2006).

[Martorell et al., 2009] Martorell, S., Nebot, Y., Villanueva, J.F., Carlos, S., Serradell, V., Pelayo, F., Mendizábal, R. An approach to integrate thermal-hydraulic and probabilistic analyses in addressing safety margins estimation accounting for uncertainties. Safety, Reliability and Risk Analysis: Theory, Methods and Applications - Proceedings of the Joint ESREL and SRA-Europe Conference, Volume 4, Pages 2827-2835, (2009).

[McLachlan et al., 2000] McLachlan, G., Peel, D. Finite Mixture Models. John Wiley & Sons Inc., New York, (2000).

[NEA, OECD, 2011] Nuclear Energy Agency, Organization for Economic Co-operation and Development. Technology and Components of Accelerator-driven Systems. Workshop Proceedings, Karlsruhe, Germany, 15-17 March, (2011).

[Negrini et al., 2003] Negrini, A., Proto, G. Operating Requirements for a Proton Beam Accelerator to Couple with a Subcritical System. Utilisation and Reliability of High Power Proton Accelerators, Nuclear Science, Workshop proceeding, Santa Fe, New Mexico, USA,pp. 259-287, 12-16 May 2002. Organisation for Economic Co-operation and Development, (2003).

[NUREG CR-6042, USNRC, 1994] NUREG CR-6042, U.S. Nuclear Regulatory Commission: Perspectives on Reactor Safety, March (1994).

[Nutt et al., 2004] Nutt, W.T, & Wallis, G.B. Evaluation of Nuclear Safety from the outputs of Computer Codes in the Presence of Uncertainties. Reliability Engineering and System Safety, Vol. 83, Issue 1, pp. 57-77, (2004).

[ORNL, 2000] Popov, S.G., Ivanov, V.K. (Russian Research Center "Kurchatov Institute"), Cabajo, J.J., Yoder, G.L., Oak Ridge National Laboratory, Engineering Technology Division. ORNL/TM-2000/351, (2000).

[Panasiti et al., 1999] Panasiti, M.D., Lemmon, E.W., Penoncello, S.G., Jacobsen, R.T., Friend, D.G. Thermodynamic Properties of air from 60 to 2000 K at Pressures up to 2000 MPa. International Journal of Thermophysics, Vol. 20, No. 1, (1999).

[Rutt et al., 2006] Rutt, B., Catalyurek, U., Hakobyan, A., Metzroth, K., Aldemir, T., Denning, R., Dunagan, S., & Kunsman, D. Distributed Dynamic Event Tree Generation for Reliability and Risk Assessment. Challenges of Large Applications in Distributed Environments, 2006 IEEE, pp. 61-70, ISBN 1-4244-0420-7/06, (2006).

[Secchi et al., 2008] Secchi, P., Zio, E., & Di Maio, F. Quantifying uncertainties in the estimation of safety parameters by using bootstrapped artificial neural networks. Annals of Nuclear Energy, Vol. 35, No. 12, pp. 2338–2350, pp. 2399-2342, ISSN 0306-4549, (2008).

[Siu, 1994] Siu, N., Risk assessment for dynamic systems: an overview, Reliability Engineering and System Safety, 43, 43-73, 1994.

[US D.O.E., 2009] US Department of Energy: Light water reactor sustainability research and development program plan, fiscal year 2009-2013. INL/MIS-08-14918, pp. 24-32, (2009).

[U.S. NRC, 1978] U.S. Nuclear Regulatory Commission. An Acceptable Model and Related Statistical Methods for the Analysis of Fuel Densification. Regulatory Guide 1.126, Revision, 1st March, (1978).

[U.S. NRC, 1996] United States: Nuclear Regulatory Commission. Emergency Core Cooling Systems Evaluation models, Appendix K to 10, CFR Part 50, Code of Federal Regulations, NRC, Washington, DC, (1996).

[Wald, 1943] Wald, A. An extension of Wilks' method for setting tolerance limits. Annals of Mathematical Statistics 14 (1), pp. 45-55, (1943).

[Wilks, 1941] Wilks, S.S. Determination of sample sizes for setting tolerance limits. Ann. Math. Statist., Vol. 12, No. 1, pp. 91–96, (1941).

[Wilks, 1942] Wilks, S.S. Statistical prediction with special reference to the problem of tolerance limits. Ann. Math. Statist., Vol. 12, No. 4, pp. 400-409, (1942).

[Won, 1996] Won, H.G. An Anderson-Darling Goodness-of-Fit Test for the Gamma Distribution, Dept. of Industrial Engineering, Hasnsung University, (1996).

[Zio et al., 2008[a]] Zio, E., & Di Maio, F. Bootstrap and Order Statistics for Quantifying Thermal-Hydraulic Code Uncertainties in the Estimation of Safety Margins. Science and Technology of Nuclear Installations, Vol. 2008, Article ID 340164, 9 pages, (2008).

[Zio et al., 2008[b]] Zio, E., Di Maio, F., Martorell, S. & Nebot, Y., Neural networks and order statistics for quantifying nuclear power plants safety margins. Safety, Reliability and Risk Analysis: Theory, Methods and Applications, Taylor & Francis Group, London, ISBN 978-0-415-48513-5, Proceedings of ESREL 2008 Conference, Valencia, Spain, (2008).

[Zio et al., 2010] Zio, E., Di Maio, F., & Tong, J. Safety margins confidence estimation for a passive residual heat removal system. Reliability Engineering and System Safety, Vol. 95, Issue 8, pp. 828–836, (2010).

[Zio et al., 2012] Zio, E., & Di Maio, F. Needs and dreams for methodologies of Integrated Deterministic and Probabilistic Safety Analysis (IDPSA). Proceeding of IDPSA workshop, 20 November 2012, Stockholm, Sweden, (2012).

[Zio, 2014] Zio, E., Integrated deterministic and probabilistic safety assessment: Concepts, challenges, research directions, DOI: 10.1016/j.nucengdes.2014.09.004.